

OH (1720 MHz) Masers and Mixed-Morphology Supernova Remnants

F. Yusef-Zadeh

Department of Physics and Astronomy, Northwestern University, Evanston, IL 60208
(zadeh@northwestern.edu)

M. Wardle

Department of Physics, Macquarie University, NSW 2109, Australia
(wardle@physics.mq.edu.au)

J. Rho

SIRTF Science Center, California Institute of Technology, MS 220-6, CA 91125
(rho@ipac.caltech.edu)

M. Sakano

Department of Physics and Astronomy, University of Leicester, Leicester LE1 7RH, UK
(mas@star.le.ac.uk)

Received _____; accepted _____

ABSTRACT

Radio surveys of supernova remnants (SNRs) in the Galaxy have uncovered 19 SNRs accompanied by OH maser emission at 1720 MHz. This unusual class of maser sources is suggested to be produced behind a shock front from the expansion of a supernova remnant running into a molecular cloud. An important ingredient of this model is that X-ray emission from the remnant enhances the production of OH molecule. The role of X-ray emission from maser emitting (ME) SNRs is investigated by comparing the X-ray induced ionization rate with theory. One aspect of this model is verified: there is a strong association between maser emitting and mixed-morphology (MM) or thermal composite SNRs –center-filled thermal X-ray emission surrounded by shell-like radio morphology. We also present ROSAT and ASCA observations of two maser emitting SNRs: G21.8–0.6 (Kes 69) and G357.7–0.1 (Tornado).

Subject headings: ISM: Clouds—ISM: general—shock waves—supernova remnants—X-rays: ISM

1. Introduction

The interaction between supernova remnants and molecular clouds constitutes an important part of Galactic ecology. Such interactions should be common because massive stars do not drift far from their parent cloud during their short lifetime. Nearby supernova explosions are responsible for driving shocks into molecular clouds as they heat, stir, disrupt, change the chemical evolution of the cloud and possibly trigger star formation.

OH masers at 1720 MHz have recently provided powerful signatures of SNR-molecular cloud interaction sites (Frail, Goss & Slysh 1994; Wardle & Yusef-Zadeh 2002). The masers arise in dense ($\sim 10^5 \text{ cm}^{-3}$) gas with a temperature in the range 50–125 K – conditions that occur in shocked molecular gas (Elitzur 1976; Lockett, Gauthier & Elitzur 1999). The necessary OH abundance in the shocked gas ($\text{OH}/\text{H}_2 \gtrsim 10^{-6}$) is created by the dissociation of shock-produced water induced by thermal X-rays emitted from the hot gas filling the adjacent supernova remnant (Wardle 1999). Nineteen remnants (about 1 in 10) have 1720 MHz masers, and are therefore likely to be interacting with clouds (Frail *et al.* 1996; Green *et al.* 1997; Koralesky *et al.* 1998; Yusef-Zadeh *et al.* 1999). The inferred interactions have been confirmed by follow up searches for millimeter or infrared emission from hot molecular gas or from molecules produced by the rich chemistry occurring within the shock front (e.g. Reach & Rho 1998; Frail & Mitchell 1998; Reynoso & Mangum 2000; Yusef-Zadeh *et al.* 2001; Lazendic *et al.* 2002a).

A supernova remnant’s X-ray appearance is also believed to be affected by interaction with a molecular cloud or dense atomic gas (Rho & Petre 1998). The X-ray morphology of supernova remnants was originally divided into shell-like, Crab-like (plerionic), and shell-like remnants containing plerions (composite) morphologies (Seward 1985). An additional “mixed-morphology” (MM) class (sometimes called thermal composites) contains approximately 25% of X-ray detected remnants, which appear center-filled in X-rays and

shell-like at radio wavelengths (Rho 1995; Rho & Petre 1998). These remnants possess a soft thermal bremsstrahlung continuum and H-like and He-like metal lines with roughly solar abundances, characteristic of hot interstellar gas rather than shocked ejecta (Rho & Petre 1996). The interstellar gas in the interior of MM SNRs is accounted for by the passage of a supernova shock propagating into dense and possibly clumpy interstellar gas. In one model, soft thermal X-ray emission arises via the evaporation of clumps overrun by the supernova shock (White and Long 1991). Alternatively, heat conduction within a remnant expanding into a moderate-density medium reduces the internal temperature and density gradients and is responsible for their X-ray appearance (Chevalier 1999; Cui and Cox 1992; Cox et al. 1999; Shelton et al. 1999).

There are reasons to expect significant overlap of the mixed-morphology and maser-emitting classes of supernova remnants. Both are believed to arise through interaction with an adjacent molecular cloud (although MM remnants may also arise through expansion into a dense atomic region), and the soft thermal X-rays emitted from a mixed-morphology remnant appear to be a necessary ingredient for enhancing OH behind the shock front (Wardle 1999). It has been noted previously that several 1720 MHz remnants fall into the mixed-morphology class (Green *et al.* 1997).

Here we address the following two new key points related to the nature of MM and ME SNRs: First, we address the physical relationship between two different class of objects, MM and ME SNRs. Although a number of papers have previously suggested that some of the brightest and most well-known MM and ME SNRs (e.g. W28, W44 and IC 443) are physically correlated, in none of the previous studies, has an unbiased quantitative and statistical analysis of all the ME SNRs been made. Given the speculative state of this correlation in previous studies, the present analysis puts correlation of these two class of remnants on a strong footing and shows that there is statistical evidence for an association between these two classes of remnants. This correlation may imply that MM remnants

require to have dense molecular gas in their environment to explain their unusual centrally filled X-ray morphology.

Second point we address here is to test the model by Wardle (1999) who predicted that X-ray emission is one of the main ingredients responsible for production of OH molecule behind a C-type shock. In order to test this model, we searched for X-ray emission from all known SNR masers and measured X-ray ionization rate at the edge of SNR masers whose thermal spectrum and whose MM have previously been identified. We also report the first evidence of X-ray detection from the Tornado nebula and Kes 69. It should be pointed out that such an analysis to determine X-ray ionization rate associated with SNR masers have never been made previously. Our analysis gives a strong support to the mechanism responsible for production of OH masers with the implication that shock chemistry incorporating X-ray induced ionization and dissociation is important.

2. An Association between Mixed-morphology and Maser-emitting SNRs

We have examined the X-ray properties of all known ME SNRs. Among 190 SNRs that have been searched for OH (1720 MHz) maser emission, 19 detections are found in the disk and in the Galactic center (e.g. Green 1997; Yusef-Zadeh *et al.* 1999). Table 1 shows the names of all known 19 ME SNRs and their corresponding X-ray characteristics compiled from observations using ASCA, ROSAT and *Einstein* data. The X-ray and radio properties of each remnant are taken from references indicated in column ten. These ME remnants fall into three broad groups. The first group of seven have MM counterparts, the second group of eight show X-ray emission but future observations are required to determine the morphology and the spectrum of these remnants. Both groups are denoted Y in column 6. The remaining four remnants have unknown X-ray properties, either being unobserved in X-rays or their soft X-ray emission have been absorbed by intervening interstellar gas.

We note that the detection of X-ray emission from G357.7+0.1 (source 13), G21.8-0.6 (Kes 69) and G349.7+0.2 (Slane et al. 2002) in the second group of remnants are found from ASCA and ROSAT archival data. Examining GIS detector of ASCA’s archival data, a weak X-ray emission at a level of 3–3.5 σ has been detected from the head of the Tornado nebula near $\alpha = 17^h40^m10.1^s, \delta = -30^{\circ}58'8.4''$ (J2000). This position coincides within 30'' of the compact maser position associated with the Tornado nebula (Frail et al. 1996). The other remnant in the second group in Table 1 is Kes 69 which has an incomplete radio shell morphology and X-ray emission has been reported from Einstein observations (Seward 1990). Figure 1 shows contours of X-ray emission based on ROSAT PSPC observations superimposed on a grayscale NVSS radio continuum image at 20cm (Condon et al. 1998). The brightest X-ray feature lies in the interior of the radio shell surrounded by a number of X-ray blobs forming two halves of a shell-like structure. An X-ray feature is also noted to the east possibly coincident with the radio shell near $\alpha = 18^h33^m18^s, \delta = -10^{\circ}09'$ (J2000). Many of the radio and X-ray features are distributed to the south delineating a partial arc. The northern half of the radio shell is weak and is best detected in low-resolution 90cm image of Kes 69 by Kassim (1992). The cross shows the position of the OH(1720 MHz) maser associated with the remnant (Green et al. 1997).

We have extracted PSPC spectra from the entire SNR G21.8-0.6 (Kes 69) excluding the bright point source near $\alpha = 18^h32^m50.677^s, \delta = -10^{\circ}01'15''$ (J2000) and fit thermal and non-thermal models. Both models yield reduced χ^2 of 1.1, but the power law index in the non-thermal fit is negative, which is non-physical, maybe suggesting the emission is thermal. The best fit is using a thermal model (Mewe, Gronenschild and van den Oord 1985; a.k.a. "vmekal" in XSPEC) with $N_H = 2.4 \times 10^{22} \text{ cm}^{-2}$ and $kT = 1.6 \text{ keV}$. The inferred luminosity is $3.5 \times 10^{35} \text{ erg s}^{-1}$ assuming the distance of 11.2 kpc. Assuming a distance of 11.2 kpc and a geometrical mean angular size of $\approx 10'$, estimated from the distribution of X-ray image in Figure 1, the X-ray ionization rate (ζ) is estimated to be $\approx 10^{-16} \text{ s}^{-1}$. However,

there are considerable uncertainties in making this estimate including the angular size and the distribution of the X-ray emission with respect to radio emission. Other uncertainties include the distance determination ranging between 6.3 and 11.2 kpc and the spectral model due to poor spectral resolution of PSPC and the presence of multi-temperature components. Thus, the bright X-ray emission from the interior of the radio shell and a possible thermal X-ray spectrum suggest that this remnant may be a mixed-morphology SNR, but due to the poor quality of the data, future observations are required to determine the nature of this source. Similarly, better distance determination as well as X-ray morphology are needed not only for G21.8-.06 but also G349.7+0.2 in order to include them in group 1. Slane et al. (2002) have recently reported X-ray emission from G349.7+0.2 and estimated X-ray luminosity of 1.8×10^{37} erg s⁻¹ at a distance of 22 kpc. Using the angular size of 1' (6 pc), the X-ray ionization rate is estimated to be $\sim 2 \times 10^{-14}$.

At present there are no counterexamples to the conjecture that all SNRs with OH(1720 MHz) masers are mixed-morphology. Even if all of the SNRs with unknown X-ray morphology are assumed to *not* be mixed-morphology, the number of mixed-morphology remnants with 1720 MHz masers (i.e. 7) is much higher than random given that 10% of SNRs are ME (Koralesky *et al.* 1998) and that 7% of SNRs are MM (Rho & Petre 1998). We can quantify this by using a contingency table (Sokal & Rolfe 1995; see also Press et al. 1992) to test the null hypothesis that there is no association between MM and ME remnants (see Table 2). The bold entries in Table 2 give the number of SNRs broken down by presence or absence of OH(1720 MHz) masers and their X-ray properties (i.e. mixed morphology, not mixed morphology and unknown), giving six categories of remnant. The numbers for SNRs with 1720 MHz masers in the first row are derived from Table 1. The numbers for SNRs *without* 1720 MHz masers listed (in bold) in the second row of Table 2 are less certain, being based on the total of 15 MM remnants identified by Rho & Petre (1998) and their estimate that this represents about 25% of X-ray detected SNRs. However, our

results are not sensitive to these numbers, nor to the fact that only 190 of the 225 known galactic SNRs have been surveyed for 1720 MHz masers. The second entry in each of the six SNR categories is the expected number of remnants derived from the counts assuming that the maser and X-ray characteristics are completely independent of one another. Finally, the third entry gives the contribution to χ^2 , $(\text{observed-expected})^2/(\text{expected})$ from each category. The total χ^2 is 27.5 with 2 degrees of freedom, indicating that the hypothesis of independence can be rejected at the level of 1.1×10^{-6} , in other words that the two classes are associated. Most of the contribution to χ^2 comes from the 7 remnants in the first group - by chance one would expect 1.5. We have, of course, assumed that there is no selection bias in the observations. The most obvious bias - that X-rays observations are limited by interstellar absorption, whereas radio observations are not, does not cause obvious problems.

3. X-ray Shock Chemistry

We have also examined whether the X-ray emission from the individual remnants in the first group of Table 1 is sufficient to dissociate water molecules behind a C-type shock front and produce the OH column necessary for OH(17200 MHz) masers. The X-ray induced ionization rate in the gas should be $\zeta \gtrsim 10^{-16} \text{ s}^{-1}$ (Wardle 1999). The X-ray ionization rate at the edge of the remnant, listed in column 9, is estimated from the total X-ray luminosity of individual remnants using $\zeta = N_e \sigma F_X$, where $N_e = 30 \text{ keV}^{-1}$ is the mean number of primary and secondary electrons generated per unit energy deposited by X-rays, $\sigma \approx 2.6 \times 10^{-22} \text{ cm}^2$ is the photoabsorption cross section per hydrogen nucleus at 1 keV, and $F_X \approx L_X/4\pi r^2$ is the X-ray intensity at the edge of the remnant. The values of the ionization rate (ζ) of ME SNRs with MM counterparts is consistent with the predicted range within a factor of few.

Significant uncertainty arises from the asymmetric and clumpy distribution of the X-ray emission, differential extinction across the face of the remnant and the estimated column density of neutral gas along the line of sight based on fitted spectrum of the remnant. One example of this uncertainty is as follows. Two studies of G359.1-0.5 based on ASCA and ROSAT give different values of hydrogen column and soft X-ray flux (Egger and Sun 1998; Bamba et al. 2000). The unabsorbed X-ray flux differs by a factor of 25 due to different thermal plasma models used by these authors. Both studies give low value of X-ray flux at the edge of the remnant, F_x in column 8. We selected the higher flux values given by Egger and Sun (1998) because G359.1-0.5 is surrounded by two bright hard X-ray sources and hard X-ray emission from the Galactic center region. Source confusion may contaminate the background subtraction, particularly the low-resolution ASCA data despite the careful analysis of Bamba et al. (2000). G359.1-0.5 is a highly symmetric shell-type SNR at radio wavelengths whereas the X-ray emission is concentrated mostly to one side of the interior. Reducing the size of X-ray emission by a factor of two increase F_x by a factor of four which is consistent with the predicted value of $3 \times 10^{-16} \text{ s}^{-1}$ (Wardle 1999).

4. Implications

The strong association between MM and ME remnants plus the fact ME remnants are interacting with molecular clouds suggest that many MM remnants are created by the interaction with a dense cloud or the denser-than average environment surrounding molecular clouds (White and Long 1991; Chevalier 1999; Shelton et al. 1999). The MM remnants without OH(1720 MHz) masers may be formed as a result of expansion into a moderate density medium (Shelton et al 1999). Alternatively, all MM remnants could arise from interaction with molecular clouds, with masers failing to arise because of the restricted physical conditions under which compact maser emission is formed (Lockett *et al.* 1999) or

the masers could simply be beamed away from the line of sight. These effects could explain the lack of ME counterparts for eight of the MM SNRs, tabulated by Rho *et al.* (1998). It would be useful to examine the eight MM remnants without maser emission for other, more generic, signatures of molecular cloud interactions such as OH absorption or emission from hot H₂ at 2 μm.

Within the uncertainty of our heterogeneous samples, the estimated X-ray-induced ionization rates are sufficient to enhance the OH behind shock waves driven into molecular clouds by SNRs (Wardle 1999). It appears that the ionization rates in molecular clouds adjacent to SNRs, $\sim 3 \times 10^{-16} \text{ s}^{-1}$, are 10–30 times greater than generally adopted. It would be interesting to consider the consequences for chemistry within the clouds. In particular, future millimeter, submillimeter and infrared observations should be useful to determine the role of X-ray shock chemistry in the ME and MM SNRs.

Acknowledgments: We are grateful to Mike Wheatland for suggesting the contingency table analysis and to Jasmina Lazendic for discussing her results prior to publication. We also thank the referee for useful comments. MS and FYZ acknowledge partial support from Japan Society of the Promotion of Science and NASA, respectively.

REFERENCES

- Asaoka, I. & Aschenbach, B. 1994 *A&A*, 284, 573
- Bamba, A. Yokogawa, J., Sakano, M. & Koyama, K. 2000, *PASJ*, 52, 259
- Chevalier, R.A. 1999, *ApJ*, 511, 798
- Claussen, M.J., Frail, D.A., Goss, W.M., & Gaume, R.A. 1997, *ApJ*, 489, 143
- Condon, J. J., Cotton, W. D., Greisen, E. W., Yin, Q. F., Perley, R. A., Taylor, G. B. & Broderick, J. J. 1998, *AJ*, 115, 1693
- Cox, D.P., Shelton, R.L., Maciejewski, W., Smith, R., Plewa, T. et al. 1999, *ApJ*, 524, 179
- Cui, W. & Cox, D.P. 1992, *ApJ*, 178, 159
- Elitzur, M. 1976, *ApJ*, 203, 124
- Egger, R. & Sun, X. 1998, in the Proc. of IAU Colloq. No. 166, eds: Brietschwerdt, M.J., Freyberg, J. and J. Trumper, *Lecture Notes in Physics 506* (Springler-Verlag, Berlin) p417
- Frail, D. A., Goss, W. M., Reynoso, E. M., Giacani, E.B., Green, A. J. & Otrupcek, R. 1996, *AJ*, 111, 1651
- Frail, D.A., Goss, M.W. & Slysh, V.I. 1994, *ApJ*, 424, L111
- Green A.J., Frail, D.A., Goss, W.M. & Otrupcek, R. 1997, *AJ*, 114, 2058
- Kassim, N. 1992, *AJ*, 103, 943
- Koo, B.-C., Kim, K.T., & Seward, F.D. 1995, *ApJ*, 447, 211
- Koralesky, B., Frail, D.A., Goss, W.M., Claussen, M.J. & Green, A.J. 1998, *AJ*, 116, 1323
- Lazendic, J.S. et al. 2002b, in preparation
- Lazendic, J.S., Wardle, M., Burton, M.G., Yusef-Zadeh, F., Whiteoak, J.B., Green, A.J. *et al.* 2002a, *MNRAS*, 331, 537

- Leahy, D.A. 1989, A&A, 216, 193
- Lockett, P., Gauthier, E. & Elitzur, M. 1998, ApJ, 511, 235
- Maeda, Y., Baganoff, F. K. Feigelson, E. D., Morris, M., Bautz, M. W. et al. 2002, ApJ, 570, 671
- Mewe, R., Gronesechild, E.H.B.M., & ven den Oord, G.H.J. 1985, A&AS, 62, 197
- Press, W. *et al.* 1992, Numerical Recipes in Fortran (Cambridge University Press: Cambridge)
- Reach, W. T. & Rho, J. 1998, ApJ, 507, L93
- Reynoso, E.M. & Mangum, J.G. 1999, ApJ, 511, 798
- Rho, J. 1995, An X-ray study of composite supernova remnants, PhD thesis, University of Maryland
- Rho, J. & Berkowski, K.J. 2002, ApJ (in press)
- Rho, J. & Petre, R. 1996, ApJ, 467, 698
- Rho, J. & Petre, R. 1998, ApJ, 503, L167
- Rho, J. Petre, R. Schlegel, E.M. & Hester, J.J. 1994, ApJ, 430, 757
- Seward, F.D. 1985, Comments Astrophys. XI, 1, 15
- Seward, F.D. 1990, ApJS, 73, 781
- Sidoli, L., Merghetti, S., Treves, A., Parmer, Turolla, R. et al. 2001, A.&A., 372, 651
- Shelton, R.L., Donald. P. Cox, D.P., Maciejewski, Smith, W. et al. 1999, ApJ, 524, 192
- Slane, P., Chen, Y., Lazendic, J. & Hughes, J. 2002, ApJ (in press).
- Sokal, R. R. & Rohlf, F. J. 1995, Biometry : the principles and practice of statistics in biological research (New York: W.H. Freeman)
- Sugizaki, M., Mitsuda, K., Kaneda, H., Matsuzaki, K., Yamauchi, S. et al. 2001, 134, 77

Wardle, M. 1999, ApJ, 525, L101.

Wardle, M. & Yusef-Zadeh, F. 2002, Science, 296, 2350

White, R.L. & Long, K.S. 1991, ApJ, 373, 543

Yusef-Zadeh, F., Uchida, K.I., & Roberts, D.A. 1995, Science 270, 1801

Yusef-Zadeh, F., Roberts, D.A., Goss, W.M., Frail, D.A. & Green, A. 1996, ApJ 466, L25

Yusef-Zadeh, F., Roberts, D.A., Goss, W.M., Frail, D.A. & Green, A. 1999, ApJ, 512, 230.

Yusef-Zadeh, F., Stolovy, S. R., Burton, M., Wardle, M., Ashley, M. C. B. 2001, ApJ, 560,
749

Fig. 1.— Contours of X-ray emission based on ROSAT PSPC observations are superimposed on a grayscale radio continuum image of Kes 69 based on NVSS observations at 20cm. The cross coincides with the position of OH(1720 MHz) maser at $v_{LSR} = 69.3 \text{ km s}^{-1}$ (Green et al. 1997).

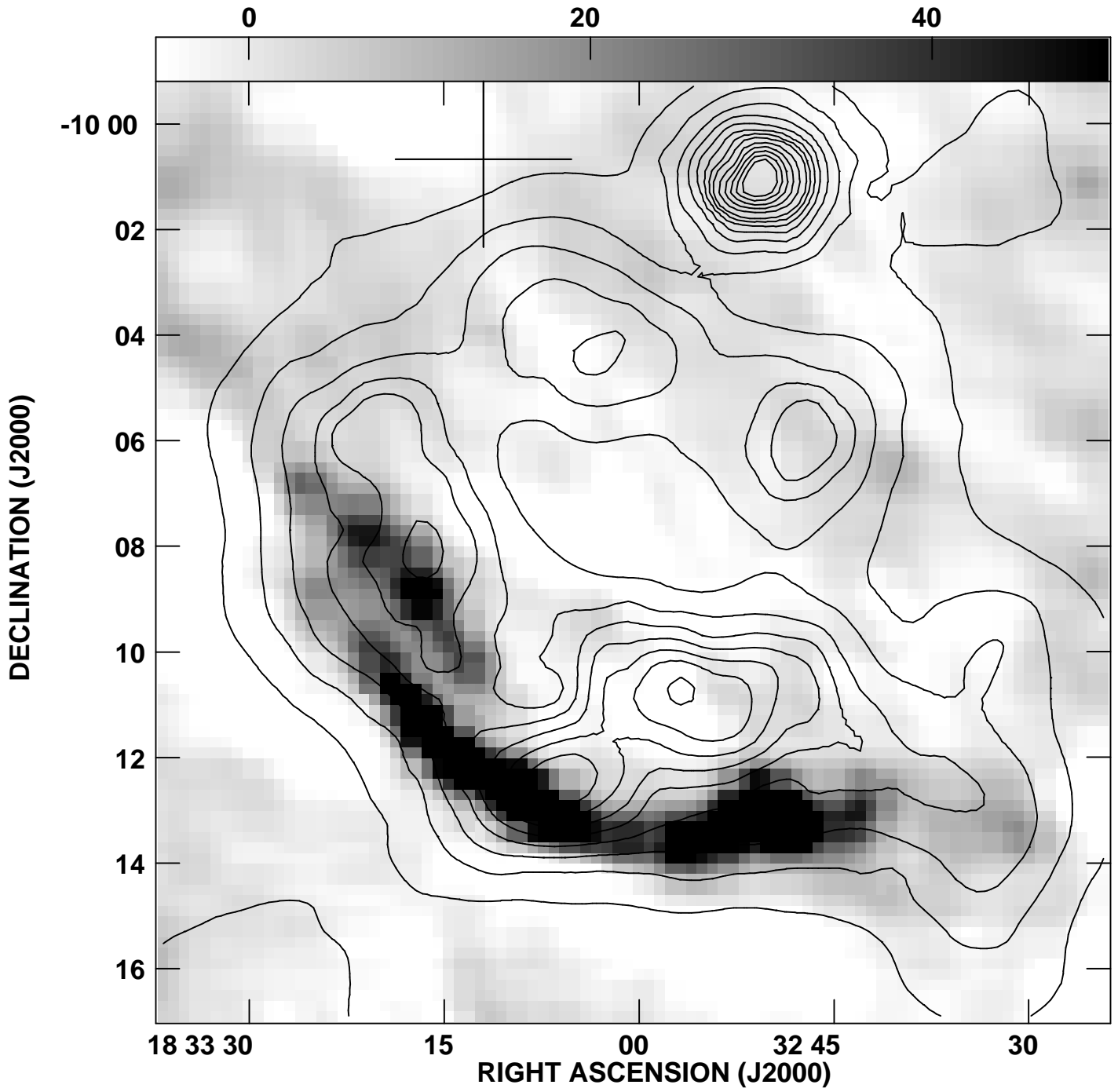


Table 1: A List of known OH (1720 MHz) Maser Emitting (ME) SNRs

Source number	SNR name	θ^a ($^{\circ}$)	D^b (kpc)	r^c (pc)	X-ray ^d	L_X^e (10^{35}) erg s ⁻¹	F_x^f (10^{-5}) erg s ⁻¹ cm ⁻²	ζ^g (10^{-16}) (s ⁻¹)	Ref ^h
1	G0.0+0.0 (Sgr A East)	2.5	8.5	3	Y	0.8	8	3.9	1, 2
2	G6.4-0.1 (W28)	42	1.8	22	Y	0.6	4.7	2.3	3, 4
3	G31.9-0.0 (3C391)	8	9	10.5	Y	17	13	6.3	5, 6
4	G34.7-0.4 (W44)	30	3	13	Y	19	9.3	4.5	4, 7
5	G49.2-0.7 (W51C)	23	6	20	Y	86	18	8.8	8, 9
6	G189.1+3.0 (IC 443)	50	1.5	11	Y	11	7.5	3.6	4, 10
7	G359.1-0.5	10	8.5	12	Y	2	1.2	0.6	11, 12
8	G1.05-0.1 (Sgr D)	8	8.5	–	Y	–	–	–	2, 14
9	G16.7+0.1	4	2/14	–	Y	–	–	–	9, 15
10	G21.8-0.6 (Kes 69)	14	11.2	–	Y	–	–	–	9, 17
11	G349.7+0.2	2	> 11	–	Y	–	–	–	6, 15, 19
12	G357.7+0.3 (Square)	24	6.4	–	Y	–	–	–	2, 13
13	G357.7-0.1 (Tornado)	5	>6	–	Y	–	–	–	2, 17
14	G337.8-0.1 (Kes 41)	5	12.3	–	Y	–	–	–	16,18
15	G346.6-0.2	8	5.5/11	–	Y	–	–	–	16,18
16	G1.4-0.1	10	8.5	–	–	–	–	–	2
17	G32.8-0.1(Kes 78)	20	5.5/8.5	–	–	–	–	–	16
18	G337.0-0.1 (CTB 33)	3	11	–	–	–	–	–	6
19	G348.5+0.1 (CTB 37A)	10	11	–	–	–	–	–	6

^a the geometrical mean of the angular diameter (θ); ^b the distance to the remnant (D); ^c the radius $r = 0.5 \times D \times \theta$; ^d X-ray detection (Y); ^e the X-ray luminosity (L_x); ^f unabsorbed X-ray flux at edge of the remnant $F_x \approx L_x / 4 \pi r^2$; ^g estimated ionization rate $\zeta = 30 / keV \times 2.6 \times 10^{-22} \times F_x$

^h References: 1) Maeda et al. (2002); 2) Yusef-Zadeh et al. (1999); 3) Rho & Borkowski (2002); 4) Claussen et al. (1997); 5) Rho and Petre (1996); 6) Frail et al. (1996); 7) Rho et al. (1994); 8) Koo et al. (1995); 9) Green et al. (1997); 10) Asaoka & Aschenbach (1994); 11) Yusef-Zadeh et al. (1995); 12) Egger & Sun (1998); 13) Leahy (1989); 14) Sidoli et al. (2001); 15) Sugizaki et al. (2001); 16) Koralesky et al. (1998); 17) this work; 18) Lazendic et al. (2002b); 19) Slane et al. (2002)

Table 2. Contingency table: presence of OH (1720 MHz) SNR masers vs mixed morphology (MM) SNRs

OH(1720 MHz) masers	# of MM SNR			Other			# of unknown			Total
Masers present	7	1.5	20.2	0	4.5	4.5	12	13	0.08	19
Masers absent	8	13.5	2.2	45	40.5	0.5	118	117	0.009	171
Total	15			45			130			190